9-7-2005

Characterization of a Novel Filarial Serine Protease Inhibitor, Ov-SPI-1, from Onchocerca volvulus, with Potential Multifunctional Roles During Development of the Parasite

Louise Ford
Laboratory of Molecular Parasitology

David B. Guiliano
Imperial College of Science and Technology

Yelena Oksov
Laboratory of Electron Microscopy

Asim K. Debnath
Laboratory of Molecular Modeling & Drug Design

Jing Liu
Institute of Evolutionary Biology

See next page for additional authors

THE JOURNAL OF BIOLOGICAL CHEMISTRY VOL. 280, NO. 49, pp. 40845–40856, December 9, 2005

Characterization of a Novel Filarial Serine Protease Inhibitor, *Ov*-SPI-1, from *Onchocerca volvulus*, with Potential Multifunctional Roles during Development of the Parasite*

Received for publication, April 22, 2005, and in revised form, September 7, 2005 Published, JBC Papers in Press, September 26, 2005, DOI 10.1074/jbc.M504434200

Louise Ford[‡1], David B. Guiliano[§1,2], Yelena Oksov[¶], Asim K. Debnath[‖], Jing Liu[‡], Steven A. Williams[**], Mark L. Blaxter[‡‡], **and Sara Lustigman[‡3]**

*From the [‡]Laboratory of Molecular Parasitology, the [¶]Laboratory of Electron Microscopy, and the [‖]Laboratory of Molecular Modeling & Drug Design, Lindsley F. Kimball Research Institute, New York Blood Center, New York, New York 10021, the [§]Molecular and Biochemical Parasitology Group, Division of Cell and Molecular Biology, Imperial College of Science and Technology, London SW7 2AY, United Kingdom, the **Clark Science Center, Smith College, Northampton, Massachusetts 01063, and the [‡‡]Institute of Evolutionary Biology, University of Edinburgh, King's Buildings, Edinburgh EH9 3JT, United Kingdom*

A novel filarial serine protease inhibitor (SPI) from the human parasitic nematode *Onchocerca volvulus*, *Ov*-SPI-1, was identified through the analysis of a molting third-stage larvae expressed sequence tag dataset. Subsequent analysis of the expressed sequence tag datasets of *O. volvulus* and other filariae identified four other members of this family. These proteins are related to the low molecular weight SPIs originally isolated from *Ascaris suum* where they are believed to protect the parasite from host intestinal proteases. The two *Ov-spi* transcripts are up-regulated in the molting larvae and adult stages of the development of the parasite. Recombinant *Ov*-SPI-1 is an active inhibitor of serine proteases, specifically elastase, chymotrypsin, and cathepsin G. Immunolocalization of the *Ov*-SPI proteins demonstrates that the endogenous proteins are localized to the basal layer of the cuticle of third-stage, molting third-stage, and fourth-stage larvae, the body channels and multivesicular bodies of third-stage larvae and the processed material found between the two cuticles during molting. In *O. volvulus* adult worms the *Ov*-SPI proteins are localized to the sperm and to eggshells surrounding the developing embryos. RNA interference targeting the *Ov-spi* genes resulted in the specific knockdown of the transcript levels of both *Ov-spi-1* and *Ov-spi-2*, a loss of native proteins, and a significant reduction in both molting and viability of third-stage larvae. We suggest the *Ov*-SPI proteins play a vital role in nematode molting by controlling the activity of an endogenous serine protease(s). The localization data in adults also indicate that these inhibitors may be involved in other processes such as embryogenesis and spermatogenesis.

The cuticle is an extracellular hydroskeleton that overlays the hypodermis of all nematodes. Most nematodes molt their cuticles four times during pre-adult development. Although being fairly inert and structurally robust, the cuticle is also permeable to small compounds and expands during growth periods between molts (1). A number of enzymes have been implicated in the shedding of old cuticles and the remodeling process that occurs as the new cuticle develops (2–8). Proteolytic enzymes have been shown to play a vital role in these processes, and inhibitor studies and rational cloning strategies have identified several nematode proteases whose functions are required for molting (9–11).

To identify novel filarial proteins involved in the molting process, we adopted a transcriptomics approach. Thousands of expressed sequence tags (ESTs)[4] have been sequenced from cDNA libraries constructed from the infective third-stage larvae (L3) and molting L3 (mL3) of the human filarial nematode *Onchocerca volvulus* (12, 13). Analysis of these datasets identified novel cysteine proteases involved in the molting process (14, 15). Also identified in these analyses was an *O. volvulus* small molecular weight serine protease inhibitor (SPI) with similarities to other nematode SPI; *Ascaris suum* chymotrypsin/elastase inhibitors and hookworm factors VII and Xa inhibitors (12, 16, 17).

Protease inhibitors play a variety of important biological roles by controlling endogenous and exogenous proteolytic activities. In parasitic nematodes they have been implicated in the parasite's survival within the host by inhibition of exogenous host proteases normally found in their preferred microenvironments (18–22), the inhibition of enzymes found in plasma or secreted from immune effector cells (17, 23–25), and the modulation of immune responses (26–29). Their endogenous roles have been less studied. It has been postulated that proteases involved in the molting process would be controlled by maturation (through removal of inhibitory pro-regions) or via endogenous protease inhibitors. In *O. volvulus* a cystatin-like cysteine protease inhibitor, onchocystatin or *Ov*-CPI-2, has been identified, which localized to the cuticle of molting nematodes and developing embryos (30). It has been suggested that it might play a role in modulating the activity of cysteine proteases required for the L3 to fourth-stage larvae (L4) molt or eggshell morphogenesis in embryos. We now present data indicating that the SPI identified in the molting EST dataset belongs to a family of proteins that play vital roles in the *O. volvulus* L3 to L4 molt and are

* The costs of publication of this article were defrayed in part by the payment of page charges. This article must therefore be hereby marked "*advertisement*" in accordance with 18 U.S.C. Section 1734 solely to indicate this fact.

The nucleotide sequence(s) reported in this paper has been submitted to the GenBank™/EBI Data Bank with accession number(s) DQ013154, DQ013161, DQ011671, and DQ011672.

[1] Both authors contributed equally to this work.

[2] Funded by the Wellcome Trust. Work in Edinburgh was funded by the UK Medical Research Council. Initial work at Smith College by D. B. G. was funded by a Hampshire College Division III Howard Hughes Medical Institute Award and the Edna McConnell Clarke Foundation.

[3] To whom correspondence should be addressed: Laboratory of Molecular Parasitology, Lindsley F. Kimball Research Institute, New York Blood Center, 310 East 67th St., New York, NY 10021. Tel.: 212-570-3119; Fax: 212-570-3121; E-mail: slustigman@nybloodcenter.org.

[4] The abbreviations used are: EST, expressed sequence tag; L2, second-stage larvae; L3, third-stage larvae; mL3, molting third-stage larvae; L4, fourth-stage larvae; Mf, microfilariae; AM, adult male; AF, adult female; *Ov*, *O. volvulus*; *Bm*, *B. malayi*; *Di*, *D. immitis*; *Ls*, *L. sigmodontis*; SPI, serine protease inhibitor; TIL, trypsin inhibitor-like; IC/E, inhibitor of chymotrypsin/elastase; BLAST, basic local alignment search tool; RNAi, RNA interference; dsRNA, double-stranded RNA; AMC, 7-amino-4-methylcoumarin; Suc, succinyl; Z, benzyloxycarbonyl; MTT, 3-[4,5-dimethylthiazol-2-yl]-2,5-diphenyltetrazolium bromide; aa, amino acid(s).

suggested to be involved in other processes such as embryogenesis and spermatogenesis.

EXPERIMENTAL PROCEDURES

Identification and Cloning of the Filarial Serine Protease Inhibitor Genes, Ov-spi-1, Ov-spi-2, Bm-spi-1, Di-spi-1, and Ls-spi-1—Analysis of ESTs from an *O. volvulus* mL3 cDNA expression library (SL96MLW-OvmL3) identified a potential serine protease inhibitor (*Ov-spi-1*, *O. volvulus* clusters OVC00017 and OVC03875), which is highly expressed in the mL3 (12). Subsequent BLAST (31) searches of the *O. volvulus* EST dataset revealed a second closely related sequence, which has been designated *Ov-spi-2*. BLAST searches of other filarial EST datasets identified further members of this gene family in *Brugia malayi*, *Dirofilaria immitis*, and *Litomosoides sigmodontis*. Representative EST clones for *Ov-spi-1* (cDNA clone SWOv3MCA025SK, GenBank™ accession AA294761), *Ov-spi-2* (SWOv3MCA738SK, AA294327), *Bm-spi-1* (kb65g12.y1, CB338347; and SWYACAL06G12SK, AW874776), *Di-spi-1* (ke26b11.y1, BQ456080), and *Ls-spi-1* (Ls_AM1_09G07_T7, CD203523) were obtained from the Blaxter laboratory (University of Edinburgh, Edinburgh, UK), the Filarial Genome Project Network repository (Smith College, Northampton, MA), or the Genome Sequencing Center Washington University (St. Louis, MO). The plasmid inserts were fully sequenced on both strands using both vector-specific and gene-specific primers. The confirmed EST sequences have been deposited in GenBank™ (*Ov-spi-1*, DQ011671; *Ov-spi-2*, DQ011672; *Bm-spi-1*, DQ013154; *Di-spi-1*, DQ013156; and *Ls-spi-1*, DQ013157).

The genomic sequences of the filarial *spi* genes were obtained by PCR amplification from total genomic DNA from each species using Long Range Taq (Stratagene, La Jolla, CA) and gene-specific primers (Bm-spi-1.F2: 5′-CACATTTGTAAACTGCTGAGAAG-3′; Bm-spi-1.R2: 5′-CTAAAACTTTTATCGACTGAATAC-3′; Ls-spi-1.F1: 5′-ATCAGAAATTACAAAGAGAATAG-3′; Ls-spi-1.R1: 5′-ATTGAACTCTCACATTTCGATGA-3′; Di-spi-1.F1: 5′-TATAAAACAATGAAAAGTAAG-3′; and Di-spi-1.R1: 5′-GCATATTTTATCTACCGTTTGGG-3′). PCR fragments were gel-purified (Qiagen kit, Qiagen Inc., Valencia, CA) and cloned into pCR4-TOPO vector (Invitrogen). For each fragment clones were selected and fully sequenced using vector- and gene-specific primers.

Sequence and Phylogenetic Analysis of the Filarial SPI Sequences—The five filarial SPI peptide sequences were compared with each other and the public datasets (NCBI GenBank™, pFam, SMART) using BLAST and ClustalX (www.sanger.ac.uk/Software/Pfam/and smart.embl-heidelberg.de/) (31–34). The inhibitory domain identified within the filarial SPIs has been designated TIL (trypsin inhibitor-like) within PFAM (PF01826). The previously identified members isolated from *A. suum* have been assigned to MEROPS proteinase inhibitor family I8 and I40, clan IA and I- (35). For the purpose of this study we limited our analysis to the nematode TIL domain containing proteins found in GenBank™ and did not include any additional nematode TILs found in the non-filarial nematode EST datasets. The sequences included in this study include the four filarial SPI sequences (ONCVU_SPI_1, BRUMA_SPI_1, DIRIM_SPI_1, LITSI_SPI_1), eleven predicted *Caenorhabditis elegans* proteins (36) containing a single TIL domain (CAEEL_C25E10_10, AAA92315; CAEEL_C10G8_4, AAB09171; CAEEL_C53B7_2, AAC48275; CAEEL_F32D8_3, T21654; CAEEL_F36H9_4, AAO12440; CAEEL_K05F1_10, AAA68717; CAEEL_K07A1_6, CAB03176; CAEEL_R10H1_4, AAM97992; CAEEL_T01D3_6 T21772; CAEEL_T06E6_10, CAB03319; and CAEEL_Y26D4A_12, CAE17955), three *A. suum* sequences (ASCSU_ATI, P19398; ASCSU_IC/E-1, P07851; and ASCSU_IC/E-2–5, P07852), five *Ancylostoma caninum* sequences (ANCCA_APc2, AAC47080; ANCCA_APc3, AAP57305; ANCCA_APc4, AAP82926; ANCCA_APc5, AAC47082; ANCCA_APc6, AAC47081), two *Ancylostoma ceylanicum* sequences (ANCCE_AP1, AAK81733 and ANCCE_AP2, AAD51336), three *Anisakis simplex* sequences (ANISI_SPI_1, O77416; ANISI_SPI_2, O77417; and ANISI_SPI_3, O77418), and two sequences identified in *Trichuris suis* (TRISU_TCI, AAF09189 and TRISU_CEI, AAF09190). The sequences of the thirty selected TIL inhibitory domains spanning between the first and the tenth cysteine residues were used to generate a preliminary multiple sequence alignment in ClustalX, which was subsequently optimized by hand editing. This multiple sequence alignment was used to carry out phylogenetic analyses using distance (neighbor joining) and Bayesian methods implemented in PAUP 4.0 (37) and MrBayes (38). For distance methods the significance of the resulting trees assessed by bootstrap analysis (10,000 replicants). The two *T. suis* sequences were designated as an outgroup because of their low sequence similarity to the other sequences and their lack of some of the conserved structural cysteine residues. *T. suis* is a member of the Dorylaimida family and only distantly related to the other (rhabditid) nematodes considered (39).

Homology Modeling of the Filarial Serine Protease Inhibitors—X-ray crystal structure of the ASCSU_IC/E-1 inhibitor (AsC/E-1; accession P07851) bound to porcine elastase was retrieved from the Protein Data Bank (PDB; code 1EAI) (40). Homology models of the filarial SPIs, *Ov*-SPI-1, *Bm*-SPI-1, *Di*-SPI-1, and *Ls*-SPI-1, were built based on the x-ray crystal structure of ASCSU_IC/E-1 using the automated software Modeler (41) within Quanta 2000 (Accelrys, San Diego, CA) running on a Silicon Graphics Octane with a dual R12000 processor (sgi, Mountain View, CA). The "Refine 3′" option in Modeler, which uses a conjugated gradient together with molecular dynamics by a simulated annealing technique, was used to optimize the models. Five models for each run were developed, and the model with the lowest Objective Function was selected. The resulting models were evaluated for their stereochemical properties by Procheck software (42) at 2.0 Å and by Quanta Protein Health programs within Quanta2000.

After initial modeling, each modeled inhibitor was superimposed on the x-ray crystal structure of the AsC/E-1 inhibitor, the latter was then removed, and the structure of the modeled inhibitor and elastase were merged. These steps were performed to investigate the interactions of the critical residues in the inhibitors with the elastase. The Quanta Protein Health Check revealed few close contacts of the modeled inhibitors with elastase, and high energy. Polar hydrogens were added to the model and optimized by 200 steps of the Steepest Descent method to remove the close contacts. The protein backbone was kept fixed during optimization. The structures of modeled inhibitors bound to elastase showed no further close contacts and low Charmm energies. These optimized structures were used for further analysis.

Expression and Purification of the Recombinant Ov-SPI-1 (rOv-SPI-1)—The mature serine protease inhibitor domain of *Ov*-SPI-1 (aa 15–118) was cloned in-frame into both the pProEX HTb (BamH1/HindIII sites) and the pRSET A (BamH1/EcoR1sites) expression vectors (Invitrogen) and expressed as a fusion with an N-terminal polyhistidine tag. Overexpression of the r*Ov*-SPI-1 fusion protein was as previously described with modifications (12). Briefly, expression was induced from an overnight culture of BL21 (DE3) pLysS *Escherichia coli* cells (Sigma) with isopropyl 1-thio-β-D-galactopyranoside at a final concentration of 1 mM for 3 h at 37 °C. Recombinant protein was purified by affinity chromatography on a nickel column (Probond resin, Invitrogen) according to the manufacturer's instructions and dialyzed overnight at 4 °C against phosphate-buffered saline.

Enzyme Inhibitory Activity of rOv-SPI-1—The inhibitory activity of r*Ov*-SPI-1 was tested against a panel of serine proteases. The enzymes

(Sigma) and their 7-amino-4-methylcoumarin (AMC) fluorogenic substrates used were bovine pancreatic trypsin and benzyloxycarbonyl-Gly-Pro-Arg-AMC (Bachem, Torrance, CA, Z-GPR-AMC); bovine pancreatic chymotrypsin and Suc-Ala-Ala-Pro-Phe-AMC (Calbiochem); porcine pancreatic elastase and Suc-Ala-Ala-Ala-AMC (Bachem); human leukocyte cathepsin G and Suc-Ala-Ala-Pro-Phe-AMC (Calbiochem). Chemical protease inhibitors (Sigma) were used as positive controls of enzyme inhibition (phenylmethylsulfonyl fluoride (5 mM), L-1-tosylamido-2-phenylethyl chloromethyl ketone (100 μM), 1-chloro-3-tosylamido-7-amino-2-heptanone (100 μM), EDTA (10 mM), and α_1-antitrypsin (5 μg/ml)). Phosphate-buffered saline diluted in enzyme assay buffer was used as a negative control. The reaction buffer was 100 mM Tris-HCl, at pH 8.0 for elastase, pH 8.0, and containing 100 mM $CaCl_2$ for chymotrypsin, and pH 7.5, and containing 1.6 mM NaCl for trypsin and cathepsin G. The assay conditions used were as follows: 0.5 μg of each serine protease in 50 μl was incubated with 100 μl of r*Ov*-SPI-1 (1, 2.5, 5, and 10 μg/ml; 0.1–1 μg of final amount/well) for 30 min at room temperature in 96-well black clear-bottom plates (Fisher Scientific) in appropriate buffer. After the preincubation of the enzyme and inhibitor, 50 μl of an appropriate AMC substrate solution (10 μM final concentration) was added, and the residual enzyme activity was measured by reading the fluorescence (excitation 360/40, emission 460/40) over time using the Bio-Tek FL500 fluorometer or the BMG Fluorostar plus Optima.

Expression Profile of Ov-spi-1 and Ov-spi-2 throughout the O. volvulus Life Cycle—Primers specific for *Ov-spi-1* (OvSPI1F; 5′-ACGTACGTGGATGCGGATC-3′ and OvSPI1R2; 5′-TGTTCCGATAAGTTACCG-3′) and *Ov-spi-2* (OvSPI1F; and OvSPI2R; 5′-GGAAACAAAATCTCAGCATC-3′) were used to amplify fragments from *O. volvulus* cDNA libraries. The specificity of the primers for *Ov-spi-1* and *Ov-spi-2* was confirmed by PCR using plasmid DNA encoding the full-length cDNA sequences of *Ov-spi-1* or *Ov-spi-2*. Each set of primers did not amplify the non-target *spi* transcript (data not shown). These include second-stage larvae (L2, SAW98MLW-OvL2), infective third-stage larvae (L3, SAW94WL-OvL3), molting third-stage larvae (mL3, SL96-MLW-OvmL3), adult male (AM, SAW98MLW-OvAM), adult female (AF, SAW98MLW-OvAF), and microfilariae (Mf, SAW98MLW-OvMf). The cDNA libraries were constructed by the Filarial Genome Project. PCR with primers specific to *O. volvulus* β-tubulin cDNA (TubF1; 5′-AATATGTGCCACGAGCAGTC-3′ and TubR1; 5′-CGGATACTCCTCACGAATTT-3′) was used as a constitutively expressed transcript qualitative control. The PCR conditions used were 95 °C for 3 min 1× cycle; 94 °C for 30 s, 55 °C for 30 s, 72 °C for 1 min 40× cycles; 72 °C for 10 min.

Polyclonal Sera Production and Immunolocalization of the Ov-SPI Proteins—Polyclonal sera raised against r*Ov*-SPI-1 was produced in mice using the immunization protocol previously described (43). Briefly, 6- to 8-week-old male BALB/cByJ mice were injected subcutaneously with 25 μg of r*Ov*-SPI-1 in 0.1 ml of phosphate-buffered saline with 0.1 ml of (Sigma). Mice were boosted 14 days later with 25 μg of r*Ov*-SPI-1 in Freund's complete adjuvant. Antibody specificity was screened by Western blot analysis against the r*Ov*-SPI-1 and other recombinant proteins. It was specific to r*Ov*-SPI-1 only (data not shown).

Stage-specific *O. volvulus* worms (L3, mL3, adult female, and adult male) were isolated as described previously (30, 44). Worms were fixed for 30 min in 0.25% glutaraldehyde, 1% sucrose in 0.1 M phosphate buffer, pH 7.4, and then processed for immunoelectron microscopy as previously described (30, 45). For the immunolocalization of the native parasite proteins corresponding to *Ov*-SPI, thin sections (70 nm) of embedded worms were incubated with antibodies raised against r*Ov*-SPI-1 (mouse anti-*Ov*-SPI-1), followed by incubation with rabbit anti-mouse IgG, and then incubation in a suspension of 15-nm gold particles coated with protein A (Amersham Biosciences). Pre-immune serum was used as the control.

Double-stranded RNA Preparation and RNA Interference—RNAi treatment of *O. volvulus* L3 was carried out using dsRNA as described by Lustigman *et al.* (46). The mature *Ov*-SPI-1 in pProEX HTb expression vector was used to amplify the cDNA corresponding to the region encoding mature *Ov*-SPI-1 (position 67–362), which also corresponds to bp 67–349 of the cDNA encoding *Ov*-SPI-2, using primers specific for *Ov-spi-1* (OvSPI1F; as above and OvSPI1R; 5′-CGAAATTTCATAGAGTCTTCCG-3′), and the PCR fragment was then subcloned into pCR4-TOPO vector (Invitrogen) to use as the template for RNA synthesis. The cDNA was amplified with M13 forward and M13 reverse primers (Invitrogen) and then used with either T3 and T7 RNA polymerase for the single-stranded sense or antisense RNA synthesis using the MEGAscript high yield transcription kit (Ambion Inc., Austin, TX). Large quantities of dsRNA were prepared as previously described (47). Soaking with dsRNA was performed on *O. volvulus* L3 as described (46), with modifications. Briefly, cryopreserved L3 were thawed and washed 5× with culture medium (1:1 NCTC 135 and Iscove's modified Dulbecco's media, plus 100 units/ml penicillin, 100 μg/ml streptomycin, and 2 mM L-glutamine) before their transfer to 96-well plates (5–15 larvae per well in 50 μl). Sterile dsRNA in culture medium was added in 50 μl at a final concentration of 0.5 mg/ml, and the larvae were cultured at 37 °C in a humidified 5% CO_2 incubator. After 20 h, 50 μl of culture medium was removed and 1.5×10^5 normal human peripheral blood mononuclear cells in 100 μl of complete medium (culture medium plus heat-inactivated fetal calf serum, final 10%) were added to the culture as previously described (10). Uptake of dsRNA into the parasite was examined using fluorescent-labeled Cy™3-dsRNA as previously described (46). The molting phenotype and morphology was observed under dissecting microscope every 24 h until the seventh day when the experiment was terminated. On day 7 larval viability was assessed visually after the uptake of MTT (3-[4,5-dimethylthiazol-2-yl]-2,5-diphenyltetrazolium bromide, Sigma) and its reduction into the blue formazan derivative (48), as described previously (49). Briefly, after incubation for 18 h at 37 °C, 5% CO_2, in 100 μl of 0.1% MTT, larval viability was scored as live when larvae stained blue uniformly along their entire length and dead when they remained unstained. *Ov-spi* dsRNA (targeting both *Ov-spi-1* and *Ov-spi-2* transcripts) was used as the test RNAi treatment, with negative controls being either culture medium containing RNA storage buffer or dsRNA of an unrelated *Plasmodium falciparum* gene *Pf-eba-140* (position 2914 to 3396; accession number MAL13P1.60), and a positive control corresponding to the cathepsin L of *O. volvulus*, *Ov-cpl* (position 219–984, accession number U71150), which has been shown to inhibit molting of L3 (46). Each RNAi experiment was repeated at least twice. The average molting of the control group is considered 100% of molting in each experiment, and the relative reduced molting rate of each experimental group is calculated accordingly. The results shown are the mean percent inhibition of molting in each experimental group, and the standard deviation reflects the variation between experiments.

Loss of Ov-spi-1 and -2 Transcripts and Native Ov-SPI Proteins following RNAi—Loss of *Ov-spi-1* and *Ov-spi-2* transcripts following RNAi treatment were examined by quantitative real-time PCR, where *Ov-spi* dsRNA treatment was expected to affect transcript levels of both *Ov-spi-1* and *Ov-spi-2* due to their high degree of identity. Primers used were specific for either *Ov-spi-1* (OvSPI1F2; 5′-AACTGCATTTGTGGTACTT-3′ and OvSPI1R2; as above), which were designed outside

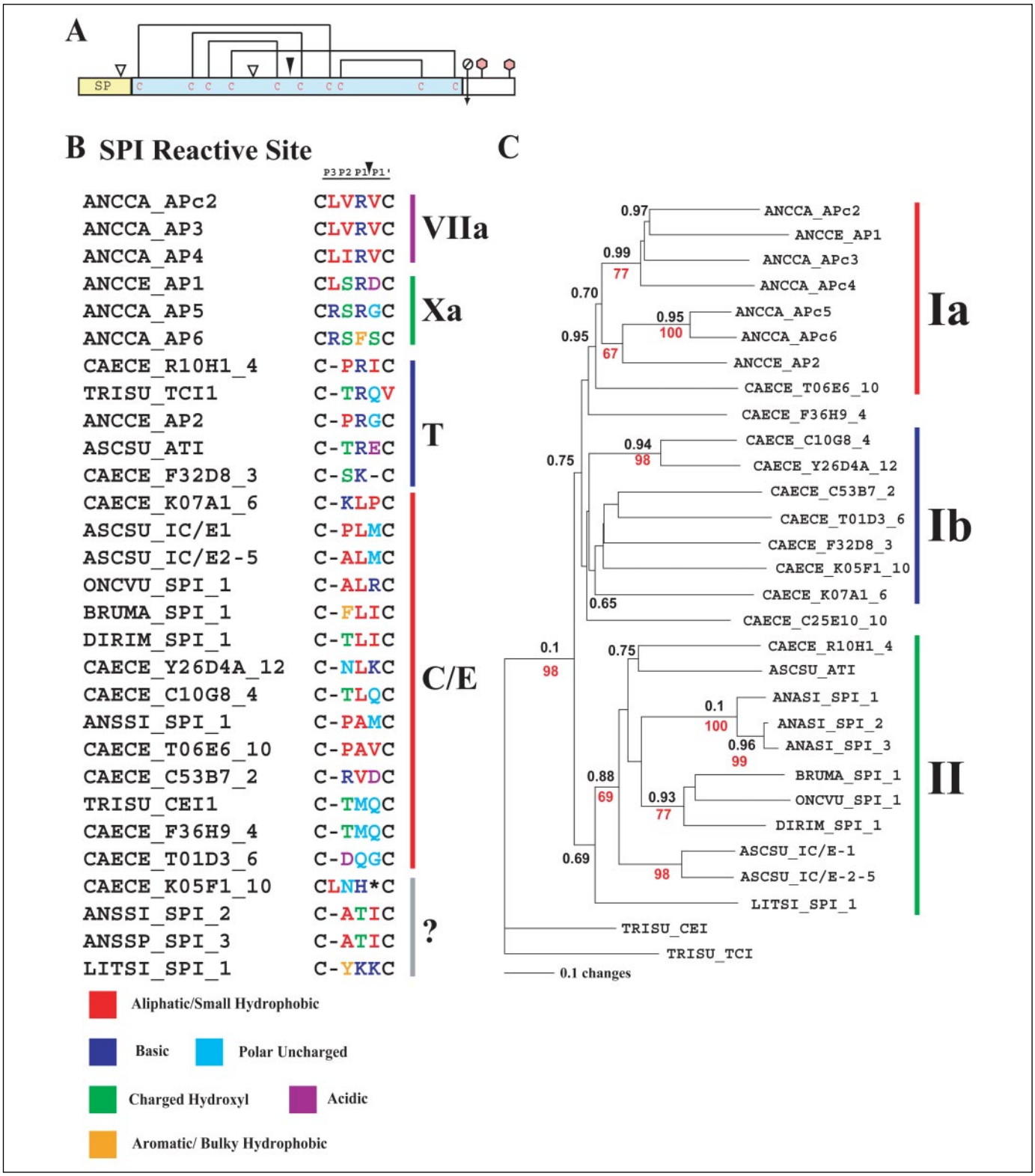

FIGURE 1. *A*, a comparison of the filarial SPI sequences. The *schematic* shows a representation of the filarial SPI-1s. The *boxes* show a schematic representation of the three different regions: signal peptide (*SP*, *yellow*); mature inhibitory (*TIL*, *blue*) domain; and C-terminal region (*white*), found in the protein sequences. The *length of the boxes* is proportional to the length of the domains in the corresponding protein group. The conserved positions of introns within the filarial SPI-1 are shown with *empty inverted triangles*. The position of the first intron in *Ls-spi-1* is shifted 3 bp forward relative to the other filarial SPIs. The positions of the ten conserved cysteines (*C*, *red*), and the disulfide bonds they are predicted to form are shown with *connecting bars*. The *closed inverted triangle* shows the position of the predicted inhibitory loop found between fifth and sixth cysteines. The *open circle* with a *bar* indicates the position of the 10-bp deletion in *Ov-spi-2*, which causes a shift in-frame and thus truncates the predicted SPI-2 protein by removing 11 aa of the C-terminal region. The *hexagons* show the two potential *N*-glycosylation sites found in *Ov*-SPI-1 with the second site also being conserved in *Bm*-SPI-1. *B*, comparison of the reactive site regions of nematode TILs. The figure shows an alignment of the inhibitory loop (residue P3 to P_1') residing between the fifth and sixth cysteines of the nematode TIL domains analyzed in this study. The residues are *colored* according to their biochemical properties and the sequences grouped according to their known or predicted substrate specificities. The groups are as follows: *VIIa*, factor VIIa; *Xa*, factor Xa; *T*, trypsin; *C/E*, chymotrypsin/elastase; and "*?*" is unknown. The *underline* indicates there is a gap in the sequence, and the *asterisk* indicates there are several additional residues before the sixth cysteine. *C*, Bayesian phylogenetic analysis of nematode SPI domains. The tree shown in this figure is a consensus built from 9,750 trees saved

the target domain of the *Ov-spi* dsRNA, or *Ov-spi-2* (OvSPI1F; as above and OvSPI2R; as above). *Ov-calponin* (Ov-9M; accession U01099), was amplified as a control housekeeping gene (Ov9F; 5′-GACGTGAGACGACGAA-3′ and Ov9R; 5′-GCACCGAATCCAGTCA-3′). ~200 RNAi soaked L3 larvae were collected after 20 h of RNAi treatment, RNA extracted as previously described (14), and first strand cDNA was generated using the SuperScript™ III first strand cDNA synthesis kit (Invitrogen) and priming with oligo(dT)20. The specific cDNA fragments were then amplified, and the copy number quantified by real-time PCR using QuantiTech™ SYBR Green PCR kit (Qiagen) and the ABI Prism 7700 Sequence Detection System. The PCR conditions used were 50 °C for 2 min, 95 °C for 15 min, followed by 43 cycles of 94 °C for 30 s, 52 °C for 30 s, and 72 °C for 45 s. To determine the copy number of each transcript within the different cDNA preparations, standard curves for *Ov-spi-1*, *Ov-spi-2*, and *Ov-calponin* were drawn based on quantitative PCR using known amounts of template DNA in a range of $10–10^6$ copies. The relative content of the transcript corresponding to *Ov-spi-1* or *Ov-spi-2* is expressed by normalizing to *Ov-calponin* and represents the ratio between *Ov-spi* copy numbers relative to *Ov-calponin*. Normalized expression in the control sample was set to 1.0, and the values for *Ov-spi-1* and *Ov-spi-2* in the RNAi-treated samples were calculated.

The effect of RNAi on the expression of the *Ov*-SPI-1/SPI-2 proteins in *Ov-spi* RNAi-treated *O. volvulus* was examined by immunoelectron microscopy. Worms were collected on day 5 and fixed for immunoelectron microscopy analysis as previously described (30, 45). Thin sections of control worms and *Ov-spi* dsRNA-treated worms were stained with antibodies raised against r*Ov*-SPI-1 as described above. The antibodies used to localize *Ov*-CPZ and *Ov*-CPL proteins in the *Ov-spi* dsRNA-treated larvae were already described (46).

Statistical Analysis—Comparison between the groups in RNA interference experiments were analyzed using the two-tailed non-parametric Mann-Whitney *U* test. A p value of < 0.05 was considered statistically significant.

RESULTS

Identification of the Filarial Serine Protease Inhibitor Genes—The cDNAs of the filarial *spi* genes encode open reading frames of 89–118 amino acids, with predicted molecular masses ranging from 9 to 13 kDa. All sequences contain a predicted N-terminal signal peptide. The predicted size of the mature SPI proteins range from 68–97 aa and 7.5–11 kDa. *Ov*-SPI-1 contains two putative *N*-linked glycosylation sites near its C terminus after the inhibitory domain (aa 105–107 and 115–117; see Fig. 1*A*). *Bm*-SPI-1 contains one potential *N*-linked glycosylation site in its C terminus (aa 93–95; Fig. 1*A*). When the *Ov*-SPI-1 sequence was searched against the *O. volvulus* EST dataset a second closely related sequence was identified, *Ov-spi-2*, which has a 10-bp deletion in the C-terminal region, relative to *Ov-spi-1*. This results in a frameshift removing 11 amino acids of the C terminus of the *Ov*-SPI-2 protein (Fig. 1*A*). *Ov*-SPI-1 exhibits 99% identity with *Ov*-SPI-2 over the first 104 amino acid residues, followed by a sequence with no identity (14 aa *Ov*-SPI-1, 2 aa *Ov*-SPI-2) due to the 11-aa deletion in the C terminus of *Ov*-SPI-2. The *Bm*-SPI-1 and *Di*-SPI-1 sequences are 57.1% and 68.1% identical to *Ov*-SPI-1, respectively. *Ls*-SPI-1 has only 33.8–40.9% identity with the other SPI family members. No putative *N*-linked glycosylation sites were identified in *Ov*-SPI-2, *Ls*-SPI-1, or *Di*-SPI-1.

The fully sequenced genomic fragments containing the predicted exons of *Ov-spi-1*, *Ov-spi-2*, *Bm-spi-1*, *Di-spi-1*, and *Ls-spi-1* have been deposited in GenBank™ (accession numbers: DQ013160, DQ013161, DQ013155, DQ013159, and DQ013158, respectively). Analysis of the fragments establishes that *Ov-spi-1* and *Ov-spi-2* are not splice variants, because the deletion does not occur at either of the verified intron splicing sites. Although the sequence of the second intron of *Ov-spi-1* and *Ov-spi-2* show a high level of sequence conservation, four single base changes and a 2-bp insertion were found in *Ov-spi-2* relative to *Ov-spi-1* genomic sequence. In addition, the 3′-untranslated region of *Ov-spi-2* has four base changes, two single base insertions, and a single 16-bp insertion relative to *Ov-spi-1*. The two intron positions in the two *Ov-spi* sequences are also conserved in *Bm-spi-1* and *Di-spi-1*, but not in *Ls-spi-1* (Fig. 1*A*).

Searches of the GenBank™ non-redundant and EST datasets revealed that TIL-like domains could be found in predicted proteins from the majority of nematode EST datasets as well as some arthropods and vertebrates. Within the nematode sequences the filarial SPIs showed the highest sequence similarity to the *A. suum* chymotrypsin and elastase inhibitors (IC/E) and the *Anisakis simplex* serine protease inhibitors (41–68% sequence similarity). Comparisons of the filarial SPI sequences to the predicted proteins of the *C. elegans* genome showed that *Ov*-SPI-1 and -2, *Bm*-SPI-1, and *Di*-SPI-1 showed the highest similarity to R10H1.4 (47–59%), whereas *Ls*-SPI-1 was most similar to C25E10.10 (52%).

The reactive site of SPIs is designated as P_3-P_2-P_1/P_1′-P_2′ (50). Fig. 1*B* shows an alignment of the reactive site loops of the filarial SPIs (*Ov*-SPI-1 and -2 amino acid sequence, CALRC; *Bm*-SPI-1, CFLIC; *Ls*-SPI-1, CYKKC; and *Di*-SPI-1, CTLIC) and other nematode SPIs with characterized protease specificities (ascarid, hookworm, and tricurid SPIs: ASCSU_IC/E-1, CPLMC; ASCSU_IC/E2–5, CALMC; ASCSU_ATI, CTREC; ANSSI_SPI_1, CPAMC; ANSSI_SPI-2/3, CATIC; ANCCA_APc2 and ANCCA_AP3, CLVRVC; ANCCA_AP4, CILRVC; ANCCA_AP5, CRSRGC; ANCCA_AP6, CRSFSC; TRISU_TCI1, CTRQC; and TRISU_CEI1, CTMQC) (51, 52). Two hookworm and ten *C. elegans* SPIs with unknown protease specificities have also been included in the alignment. The sequences have been grouped according to the characteristics of the amino acid residues found in the P_1/P_1′ positions, and their potential target enzymes were deduced from the sequences found in the characterized inhibitors. In three of the filarial inhibitors and the *Ascaris* IC/E inhibitors the amino acid leucine occupies the critical P_1 position. The P'_1 site displays more variation with aliphatic amino acids in *Ascarid* SPIs and two of the filarial SPIs (methionine in the *Ascaris* C/E inhibitors and *Anisakis* SPI-1, isoleucine in *Anisakis* SPI-2/3, *Bm*-SPI-1, and *Di*-SPI-1), and charged residues in the filarial *Ls*-SPI-1, and *Ov*-SPI-1 and -2 (lysine or arginine). The reactive site sequence of the *A. suum* trypsin inhibitor (ATI) differs with the charged amino acids arginine and glutamic acid occupying the P_1 and P_1′ reactive sites, respectively (Fig. 1*B*) (53, 54). Based on the composition of their reactive sites we speculated that the *Onchocerca* SPI-1 and -2 target a chymotrypsin/elastase-like protease. Using these criteria we also predict the majority of the *C. elegans* inhibitors included in our study (eight out of ten) will have similar target protease preferences. The remaining *C. elegans* inhibitors CAEEL_R10H1_4 and CAEEL_F32D8_3 have arginine or lysine in the P_1 position indicating that they may inhibit trypsin-like proteases.

during Bayesian analysis of the SPI protein alignment, rooted using the two *T. suis* sequences. Posterior probability values for each node >0.65 are shown in *black*. The bootstrap values (>65) of a distance analysis (neighbor joining; 10,000 replicates) of the same alignment are shown in *red*. The name includes a five-letter species identifier and the SPI gene name. Based on the results of the phylogenetic analysis a subset of the TIL domains have been divided into three groups: *Ia*, *C. elegans* T06E6.10 and hookworm TILs; *Ib*, seven *C. elegans* TILs; and *II*, *C. elegans* R10H1.4, ascarid, and filarial TILs.

Phylogenetic Analysis of the Nematode Serine Protease Inhibitor Protein Sequences—Phylogenetic analysis of the nematode TIL domains from *C. elegans*, ascarid, and filarial SPIs, using the Bayesian and neighbor joining analysis, indicates that the filarial SPI sequences are part of a large clade, which includes the previously isolated ascarid TILs from *A. suum* and *A. simplex*, as well as the *C. elegans* open reading frame R10H1.4 (Fig. 1*C*). All nodes yielding posterior probability value of >0.65 or bootstrap values of >65 are indicated. Three supported groups have been designated Ia, Ib, and II. Group I contains most of the SPI sequences derived from Clade V nematodes (39). Group Ia consists of the hookworm factors Xa and VIIa inhibitors and *C. elegans* T06E06.10, whereas the poorly supported group Ib (probability value of 0.65) consists of seven *C. elegans* sequences. Group II consists of the *C. elegans* R10H1.4, ascarid, anisakid, and filarial SPIs. The *A. simplex* and most of the filarial SPIs form their own subgroups. The overall low sequence similarity (33.8–40.9%) of *Ls*-SPI-1 to the other filarial SPIs, its unique intronic splice sites, and its exclusion from the filarial clade indicate that it may not be part of the same TIL subgroup as the other filarial sequences.

Homology-based Modeling of Ov-SPI-1 and Bm-SPI-1—The homology-based modeling of *Ov*-SPI-1, *Bm*-SPI-1, and *Di*-SPI-1 when merged with the x-ray crystal structure of porcine elastase (PDB code 1EAI), showed mutual penetration characteristics as observed in the *A. suum* chymotrypsin/elastase inhibitor bound crystal structure. The P_1 residue, Leu-31, of the inhibitor penetrates into the S_1 substrate specificity pocket, and R217A of elastase penetrates through a pore formed by the *A. suum* IC/E-1 inhibitor (40). The later penetration is a unique feature and has not been reported for any other protein inhibitor-protease complex. Although the residues in the P_1' site vary in all three inhibitors studied here, one of the key residues, Leu-31 (P_1), reported as indicative of an inhibitor of both chymotrypsin and elastase (52), is conserved in *A. suum* IC/E and in the three filarial inhibitors studied. In all of the modeled filarial structures Leu-31 can interact with the Val-216 of elastase similarly to that published for the *A. suum* IC/E interaction with elastase (40). *Ls*-SPI-1, which has lysine instead of leucine at this position, is not predicted to have this mutual penetration characteristic. The residues in the P_2 site, Pro-30 and Ala-30 in *A. suum* IC/E-1 and *Ov*-SPI-1, respectively, do not participate in any specific interactions with the residues of elastase; however, phenylalanine in the P_2 position in *Bm*-SPI-1 is predicted to interact with Val-99 in elastase. The major interactions appeared to be hydrophobic. The amino acid residues in the P_1' site at position 32, which varied in all these three structures, did not appear to have any overall effect in terms of interactions with elastase. We note that of course the nematode (and possibly host) enzymes targeted by these inhibitors will differ in sequence and fine-scale structure to the porcine elastase used in modeling and that there may be additional significant interactions with their true substrates.

Inhibitory Activity of rOv-SPI-1—The inhibitory activity of histidine-tagged r*Ov*-SPI-1 was examined by testing its ability to inhibit a variety of serine proteases (trypsin, chymotrypsin, elastase, and cathepsin G). Protease activity and specific inhibition was examined by measuring the hydrolysis of specific fluorogenic AMC substrates over time. The r*Ov*-SPI-1 inhibitor inhibited the enzymatic activity of all serine proteases screened in a dose-dependent manner (Fig. 2), specifically inhibiting elastase to the greatest extent (92.4% at the highest amount of r*Ov*-SPI-1), followed by chymotrypsin (60.2%) and cathepsin G (57.3%), and to a lesser extent trypsin (30.5%). The chemical inhibitors of serine proteases inhibited almost completely (85–100%) all of the serine proteases screened (data not shown). The specific serine protease inhibitory activity of r*Ov*-SPI-1 was confirmed using a reverse zymography technique,

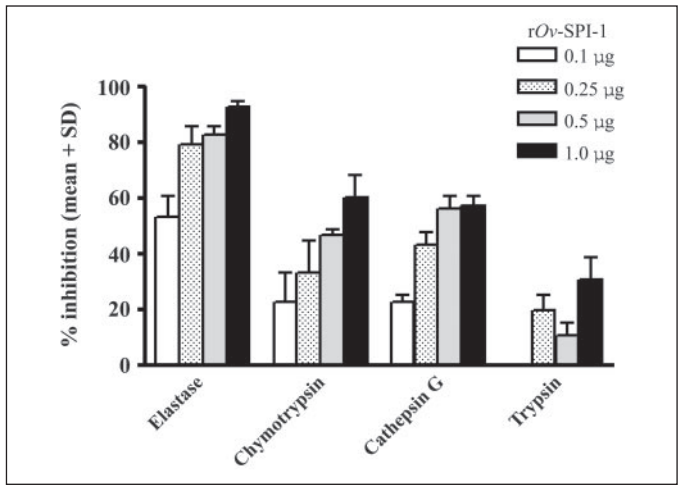

FIGURE 2. **Serine protease inhibitory activity of r*Ov*-SPI-1 is concentration dependent.** Different amounts of r*Ov*-SPI-1 were preincubated with 0.5 μg of serine proteases (elastase, chymotrypsin, cathepsin G, and trypsin) before the addition of specific fluorometric substrates, and the residual protease activity was measured. Inhibitory activity is expressed as a percentage, defined as the ratio of decreased activity relative to the no inhibitor control. All assays were performed in triplicate and values are the means of three independent experiments.

where the inhibitory activity of r*Ov*-SPI-1 was detected as a single band with an apparent molecular mass of 16 kDa (including 4 kDa for the histidine tag extension) on stained substrate gel slices, that was resistant to both elastase and chymotrypsin, but not trypsin activity (data not shown).

Profile of Ov-spi-1 and Ov-spi-2 Expression throughout the Parasites Life Cycle—Primers were designed to specifically amplify either *Ov-spi-1* or *Ov-spi-2* from different developmental stages of *O. volvulus*. PCR on *O. volvulus* stage-specific cDNA libraries indicated that the transcripts of *Ov-spi-1* are present in all life-cycle stages from microfilariae to adults, with expression increasing during molting of L3 (mL3) and in adult stages (Fig. 3). *Ov-spi-2*, however, was only found to be transcribed in L2 and the post-human-infection parasite stages (mL3 to adult) (Fig. 3). Previous analysis of the *O. volvulus* EST datasets (13, 55) indicates that *Ov-spi-1* and *Ov-spi-2* may be up-regulated in mL3 (clusters OVC00017, OVC03875, and OVC08442; 41 ESTs, 33 of which are derived from the mL3 dataset), and they represent the third most abundant transcript in the mL3 dataset (12). Because of the subtle differences between the *Ov-spi-1* and *Ov-spi-2* transcripts the EST clustering algorithms have not successfully differentiated between them. However, by specifically searching the *O. volvulus* EST datasets we identified 21 ESTs encoding *Ov-spi-1*, 11 ESTs encoding *Ov-spi-2*, and 9 that could not be assigned to either gene because of lack of sequence covering the 10-bp deletion site. In both cases the majority of ESTs were isolated from the mL3 dataset indicating that both are highly expressed at that stage.

Immunolocalization of Native Ov-SPI Proteins in O. volvulus—Specific antibodies raised against r*Ov*-SPI-1 (anti-*Ov*-SPI-1), which has 99% identity to *Ov*-SPI-2 over their first 104 amino acids, were used to detect their corresponding native proteins in the parasite. The endogenous protein corresponding to *Ov*-SPI-1 and -2 was localized by immunoelectron microscopy on sections taken from different life-cycle stages of *O. volvulus*. In L3, *Ov*-SPI-1 and -2 were present within the body channels (Fig. 4, *A* and *B*), within the multivesicular bodies (Fig. 4*B*), and in the basal layer of the cuticle (Fig. 5*B*). Intense labeling was also seen in the basal layer of the cuticle of mL3 (Fig. 4, *C* and *D*). After separation of the L3 and L4 cuticles, the *Ov*-SPI-1 and -2 proteins were present in the basal layer of both the old L3 cuticle and the new L4 cuticle (Fig. 4*D*). Interestingly, intense labeling was also observed in the processed mate-

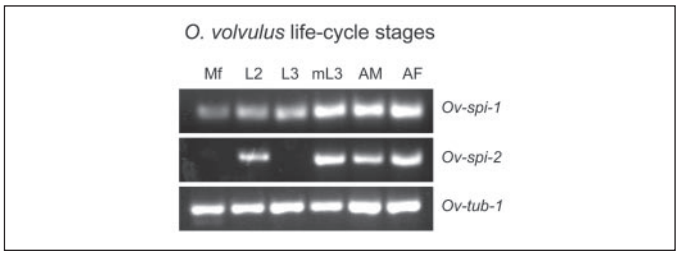

FIGURE 3. **Transcription of *Ov-spi-1* and *Ov-spi-2* through the life cycle of the parasite.** PCR was performed on *O. volvulus* cDNA libraries of microfilariae (Mf), L2, L3, molting L3 (mL3), adult female (AF), and adult male (AM). Specific primers for *Ov-spi-1*, *Ov-spi-2*, and β-tubulin (*Ov-tub-1*) were used for specific gene amplification. β-Tubulin is the normalization control for all other lanes.

rial, which appears between the L3 and L4 cuticles during molting in control larvae (Fig. 5*D*, *panel b*). No labeling was observed in the glandular esophagus. In addition, the antibodies recognized protein in eggshells surrounding developing embryos within the uterus of adult female worms (Fig. 4*E*) and strongly labeled sperm within the testis of adult male worms (Fig. 4*F*). Pre-immune sera did not cross-react with any proteins in the sections of life-cycle stages of *O. volvulus* (data not shown).

RNAi of Ov-spi in O. volvulus L3 Results in a Reduction in Larval Molting and Viability Due to a Specific Depletion of Ov-spi-1 and -2 Transcripts and Native Proteins—To determine the possible function(s) of *Ov*-SPI-1 and *Ov*-SPI-2 during molting of *O. volvulus*, RNAi was carried out to selectively interfere with *Ov-spi-1* and *-2* gene expression using dsRNA corresponding to an identical coding region of both proteins (bp 67–362). Both molting and viability were affected in *Ov-spi* dsRNA-treated *O. volvulus* L3 (Fig. 5, *A* and *B*, respectively). In comparison to 19–33% molting in the normal culture media control groups, treatment with *Ov-spi* dsRNA resulted in a 84.2% inhibition of ecdysis, which was statistically significant (Mann-Whitney *U* test, $p = 0.001$). L3 cultured in the presence of *Pf-eba-140* dsRNA showed some reduction in molting (24.7%) relative to the control. The molting of *Ov-spi* dsRNA-treated L3s was significantly reduced in comparison to the *Pf-eba-140* dsRNA-treated L3s ($p = 0.008$). Treatment with *Ov-spi-1* dsRNA significantly affected the viability of L3, which had not molted by day 7 (Fig. 5*B*), where treatment resulted in a 39.4% death of L3 relative to the control ($p = 0.032$). *Pf-eba-140* dsRNA treatment of L3 did not affect their viability (2.2% killing similar to that of control group with no dsRNA). The viability of *Ov-spi-1* dsRNA-treated L3s was significantly reduced in comparison to the *Pf-eba-140* dsRNA-treated ($p = 0.016$).

Analysis of specific gene transcript levels following RNAi treatment showed that both *Ov-spi-1* and *Ov-spi-2* transcripts in *Ov-spi* dsRNA-treated L3 were severely diminished, ~200-fold, when compared with RNAi treatment with either the negative control dsRNA (*Pf-eba-140*), or dsRNA corresponding to the *O. volvulus* cathepsin L (*Ov-cpl*) (Fig. 5*C*). Transcript levels in the medium control were comparable to those in the negative control dsRNA (data not shown). Immunoelectron microscopy demonstrated that the native *Ov*-SPI-1/SPI-2 proteins were highly reduced following *Ov-spi* dsRNA treatment (Fig. 5*D*). In normal control molting larvae *Ov*-SPI-1/SPI-2 was localized to the cuticles of both L3 and L4 (Fig. 5*D*, *panels a* and *b*), whereas in *Ov-spi* RNAi-treated L3 the labeling of *Ov*-SPI-1/SPI-2 was almost absent (Fig. 5*D*, *panel c*). Notably, larvae that did not successfully molt after *Ov-spi* dsRNA treatment exhibited incomplete separation between the L3 and L4 cuticles (Fig. 5*D*, *panel c*). Interestingly, in control larvae intense labeling was also observed in the processed material, which appears between the L3 and L4 cuticles during molting (Fig. 5*D*, *panel b*). The labeling of *Ov*-SPI-1/SPI-2 in L3 and mL3 confirmed our previous localization of the endogenous protein (Fig. 4), however, in addition the preservation of material being degraded between the cuticles during molting shows that the endogenous inhibitors are present during the degradation of cuticular material during molting. The localization of *O. volvulus* cathepsin L- and Z-like proteases, known to have an essential function during molting (46), were not affected by the *Ov-spi* dsRNA treatment (Fig. 5*D*, *panels d* and *e*).

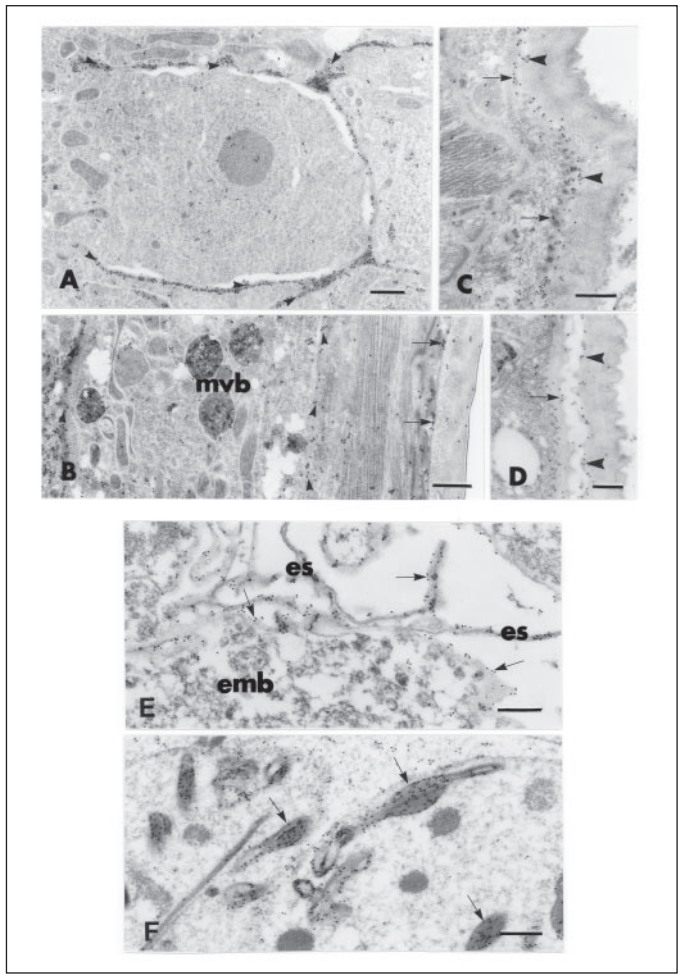

FIGURE 4. **Immunolocalization of native *Ov*-SPI-1/SPI-2 in sections of different developmental stages of *O. volvulus*.** Thin sections of *O .volvulus* L3 (*A* and *B*), mL3 (*C* and *D*), adult females (*E*), and adult males (*F*) were incubated with anti-*Ov*-SPI-1 mouse antibodies, followed by incubation with rabbit anti-mouse IgG, and then incubation with protein A coupled to 15-nm gold particles for ultrastructural localization of the native *Ov*-SPI-1/SPI-2 proteins (*bar* represents 500 nm). In L3, anti-*Ov*-SPI-1 antibodies intensely labeled the body channels (*small arrowhead*) (*A* and *B*) and multivesicular bodies (*B*; *mvb*) having a role in the early stage of molting. In mL3, antibodies reacted with proteins in the basal layer of the cuticle (*big arrowhead*) (*C* and *D*), after cuticle separation labeling was seen in the basal layer of both the old L3 (*big arrowhead*) and new L4 cuticles (*arrow*) during both early and late stages of molting (*C* and *D*, respectively). In adult stages antibodies reacted with the eggshell (*es*) surrounding developing embryos (*emb*) within the uterus of the adult female worms (*E*), and intensely labeled sperm (*sp*) within the testis of adult male worms (*F*).

DISCUSSION

Parasite-derived protease inhibitors have been shown to play a variety of roles in the survival of the parasite by inhibition of exogenous host proteases (18, 20, 29). They are also believed to control endogenous proteases involved in the development and reproduction of the parasite (30). Here we describe the identification and characterization of a novel family of low molecular weight serine protease inhibitors (SPIs), *Ov*-SPI-1 and *Ov*-SPI-2, from the human parasitic nematode *O. volvulus*.

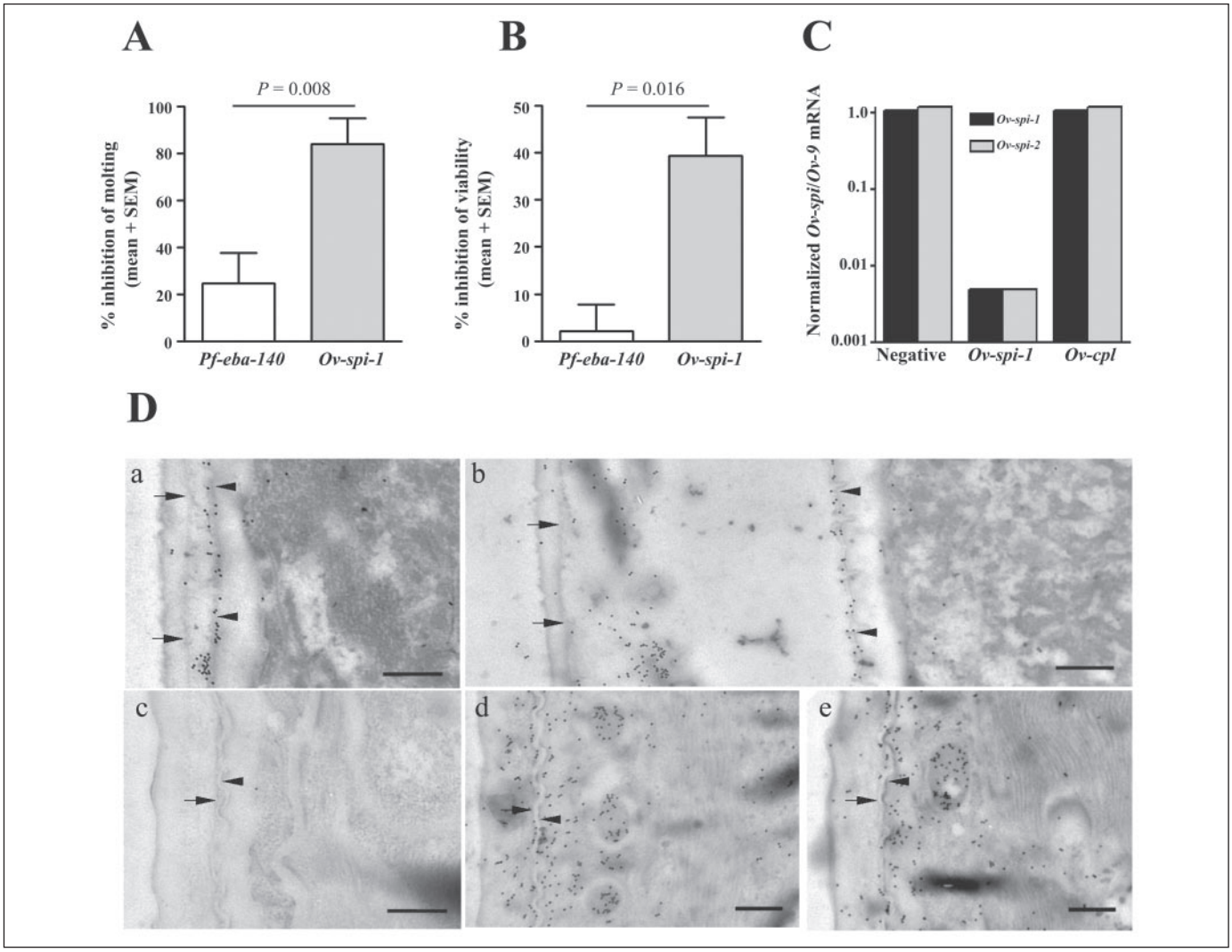

FIGURE 5. **RNAi treatment of *O. volvulus* L3 with *Ov-spi* dsRNA results in an inhibition of molting and viability due to *Ov-spi-1* and *-2* gene specific knock-down.** *O. volvulus* L3 were soaked in dsRNA at a final concentration of 0.5 mg/ml as described under "Experimental Procedures." Larvae were cultured in the presence of dsRNA for 20 h at 37 °C in humidified 5% CO_2, after which 1.5×10^5 normal human peripheral blood mononuclear cells were added and L3 were cultured for an additional 6 days. *A*, *Ov-spi* RNAi led to a significant inhibition of molting when compared with the *Pf-eba-140* dsRNA control group. The data are presented as percent inhibition relative to the normal molting control group, where the average of molting is considered 100% of molting, and the relative reduced molting rate of the two experimental groups is calculated accordingly. *B*, *Ov-spi* dsRNA-treated L3, which had not molted by day 7 showed significantly reduced viability. *C*, quantitative real-time PCR was carried out on total RNA isolated from ~200 control or RNAi-treated *O. volvulus* L3 after 20-h incubation with medium alone or dsRNA. PCR primers were specific to *Ov-spi-1*, *Ov-spi-2*, or to the control gene *Ov-calponin*. *Ov-spi* expression was normalized to *Ov-calponin* expression and normalized expression in the control group was set to 1.0. Both *Ov-spi-1* and *Ov-spi-2* RNA were depleted in *Ov-spi* dsRNA-treated L3s compared with *Pf-eba-140* or *Ov-cpl* dsRNA-treated L3s. *D*, immunoelectron microscopy was performed on control (*a* and *b*) and *Ov-spi* RNAi-treated (*c*) L3 collected on day 5 as described under "Experimental Procedures." The native *Ov*-SPI-1/SPI-2 proteins were localized to the new L4 cuticle, in-between the old and new cuticles in the control larvae (*a* and *b*), but their expression was almost completely reduced in the *Ov-spi* RNAi-treated larvae (*c*). The presence and localization of *Ov*-CPZ-1 (*d*) and *Ov*-CPL-1 (*e*) in the *Ov-spi* RNAi-treated L3s was similar as in normal mL3. The regions where the cuticles of L4 and L3 separate are marked by an *arrowhead* and an *arrow*, respectively. Each *bar* represents 500 nm.

Subsequent searching of other filarial EST datasets allowed us to identify three other members of this family from *B. malayi*, *D. immitis*, and *L. sigmodontis* (*Bm*-SPI-1, *Di*-SPI-1, and *Ls*-SPI-1, respectively). This group of low molecular weight serine protease inhibitors was first identified in *A. suum* and *A. lumbricoides* (16, 18, 51, 54) where they are believed to protect the nematode from intestinal serine proteases. Members of the family have been identified in other parasitic nematodes, including the ascaridid *A. simplex* (20, 52, 56), the strongylid hookworms *A. caninum* and *A. ceylanicum* (17, 23, 25), and the whipworm *T. suis* (21, 57). These SPIs are also believed to be involved in controlling exogenous host proteases in these nematodes. The inhibitory portions of these proteins have been designated TIL domains (trypsin inhibitor-like) within pFam. The completed *C. elegans* genome contains nineteen different genes with TIL domains (36), none of which have been purposely characterized functionally in regard to their specific roles during development. Regardless, they presumably play a variety of roles in the biology of this free-living nematode. There were no reported RNAi phenotypes associated with any of these genes in the recently published genome-wide screens (www.wormbase.org). Members of this family have been identified in arthropods such as the honeybee *Apis mellifera* (58, 59), *Drosophila melanogaster* (60), gall wasps (61), and scorpions (62). Their functions in arthropods have not yet been fully elucidated, although they are reported to be involved in determining lifespan or are components of insect venoms. TIL domain proteins have also been isolated from frogs, where they are believed to exert anti-microbial properties (63, 64). In mammals TILs have been identified in a variety of proteins such as von Willebrand factor or zonadhesin, which have roles in blood clotting and sperm gamete recognition, or adhesion (65, 66). The mammalian TILs have always been found in the context of large multidomain proteins (see entry for PF01826). This

contrasts amphibians, nematodes, and arthropods, where multiple examples of proteins just containing an N-terminal signal peptide and a single TIL domain have been identified.

We initially identified the *O. volvulus* SPIs through the analysis of a molting L3 EST dataset and subsequent PCR analysis of stage-specific cDNA libraries, which indicate that these genes are highly expressed in the molting larvae and adult datasets. Sequence analysis of the two *Ov-spi* cDNAs showed that they were closely related with only a 10-bp deletion in the C-terminal region of the open reading frame differentiating the coding sequences. Cloning and sequencing of genomic fragments indicates that *Ov-spi-1* and *Ov-spi-2* are separate genes or alleles of the same gene and not splice variants. If the *Ov-spi-1* and *Ov-spi-2* are separate genes, the high level of conservation in the intron sequences indicates that they are derived from a recent gene duplication.

Comparison of the results of the phylogenetic analysis (Fig. 1*C*) and the alignment of the nematode SPI reactive site loops (Fig. 1*B*) show that while clear relationships between the nematode SPI genes can be deduced, highly supported groups show heterogeneity in the predicted protease target specificity. This indicates that substrate specificity has not evolved in a monophyletic fashion but has remained highly dynamic perhaps in response to rapidly evolving endogenous biological processes or variable exogenous host targets (immune system or digestive enzymes). Both sequence analysis and predictive modeling indicated that the *Ov*-SPI-1 and *Ov*-SPI-2 may target chymotrypsin/elastase-like proteases. Enzyme assays of bacterially expressed recombinant *Ov*-SPI-1 confirmed that these proteins are capable of inhibiting a variety of serine proteases particularly elastase, chymotrypsin, and cathepsin G.

The potential endogenous function of the *Ov*-SPI proteins was explored indirectly using immunolocalization of the proteins during the development of the parasite. In the context of molting of L3 to L4, the native proteins were localized in L3 to the body channels, the basal layer of the cuticle, and the multivesicular bodies. The presence of the protein in the body channels of L3s suggests that it is being transported to the cuticle (67), whereas localization in the multivesicular bodies of the L3 is an important observation, because these vesicles appear to contain proteins exported to the cuticle during molting.[5] The *Ov*-SPI proteins are present in the basal layer of the cuticle of L3, the shed cuticle of L3, and the newly formed cuticle of L4. They were also localized to the material being processed and/or degraded between the cuticles during molting, suggesting that they could be involved in the inhibition of and/or regulation of one or more serine proteases that are essential for the processing/degradation of such cuticular proteins. Proteases involved in molting are thought to be active in areas beneath the basal layer of the old cuticle (2, 10). A cystatin-like cysteine protease inhibitor, *Ov*-CPI-2, has been found to have a similar localization profile as the *Ov*-SPIs. It has been suggested that *Ov*-CPI-2 controls the activity of cysteine proteases essential for molting of L3 to L4 such as *Ov*-CPZ-1 or *Ov*-CPL-1 (10, 14, 30, 46).

Although the endogenous target enzyme of *Ov*-SPI-1 is yet to be identified, a number of nematode serine proteases have been identified (20, 68–71). Serine proteases have been implicated indirectly in the molting processes of *C. elegans* (72–74). A family of subtilisin-like serine proteases, including furin and blisterase, has been identified in filariae and shown to be involve in processing of cuticular proteins (75, 76). Interestingly, *Ov*-blisterase localizes to the same regions of the cuticle in molting *O. volvulus* L3s as the *Ov*-SPI proteins,[6] suggesting that this endogenous enzyme could be a potential target of *Ov*-SPI-1 and/or *Ov*-SPI-2. In *C. elegans*, blisterase is encoded by the *bli-4* gene, which gives rise to at least nine protein isoforms by alternative splicing (72), and these enzymes are involved in the processing of hormones and structural components required for molting and the genesis of the new cuticle (72, 73). More recently it has been shown that *bli-4* is essential for molting in *C. elegans* using RNAi (77). Moreover, elastase-like serine protease activity has been detected in the secretions of *Onchocerca lienalis* L3s (78). Interestingly, serine proteases have been shown to be involved in the control of molting and larval development in insects (79–84). In addition, Kunitz-type serine protease inhibitors are constituents of the molting fluid in *D. melanogaster* where they are believed to control enzymes involved in tissue remodeling (85). Recently, using genome wide RNAi screening, it has been shown that serine protease inhibitors containing the Kunitz/bovine pancreatic trypsin inhibitor domains are also essential for molting in *C. elegans* (77). We suggest that the *Ov*-SPIs might act in a similar manner regulating the activity of a serine protease(s) involved in nematode molting. In addition to their potential role in molting, it is possible that the *Ov*-SPIs are secreted onto the surface of the nematodes cuticle or into the immediate vicinity to prevent autodigestion of its cuticle by its own secretions.

We directly addressed the function of the *Ov*-SPIs in molting by RNAi targeting of the *Ov-spi-1* and *Ov-spi-2* transcripts. When compared with the untreated control or the *Pf-eba-140* control (dsRNA treatment control) the *Ov-spi* RNAi treatment of L3s significantly inhibited molting. The treated L3s failed to shed their cuticles, displayed aberrant morphology, and reduced viability. These phenotypic differences were correlated with a loss of both *Ov-spi-1* and *Ov-spi-2* transcripts, and a specific reduction in native *Ov*-SPI-1/SPI-2 proteins. As described previously by Lustigman *et al.* (46) we noted some nonspecific toxic effect of unrelated dsRNA on molting. It is unclear what the mechanism for this nonspecific effect is, however, reverse transcription-PCR of the targeted transcripts does not indicate an indirect knockdown in their transcription. Also the protein expression of two previously characterized cysteine proteases involved in molting (*Ov*-CPL-1 and *Ov*-CPZ-1) (46) was unaffected. Off-target effects have been reported to occur in RNAi of mammalian cells (86, 87), and it possible that the AT-rich *P. falciparum* gene fragment is acting on other AT-rich transcripts found in *O. volvulus* (88). Whereas we have not specifically explored the mechanism of *Ov-spi* RNAi lethality, it is probable that it results from the unsuccessful emergence of the L4 from the old L3 cuticle.

An interesting finding in this study was the overall similarity between the RNAi phenotypes of *Ov-spi*, *Ov-cpl-1*, and *Ov-cpz-1* (46) in molting L3s. All display a similar failure in the separation of L3 and L4 cuticles. The knockdown of *Ov-spi* does not affect the transcription of the other two genes or the localization of their native proteins. It seems likely the *Ov*-SPIs regulate molting via inhibition of their unidentified endogenous target enzyme, and this activity appears to be independent of the presence of the cysteine proteases *Ov*-CPL-1 and *Ov*-CPZ-1 in the same locations. It is possible that these proteins act in independent pathways that subsequently converge when the cuticles begin separation. Alternatively, the *Ov*-SPIs could be involved in controlling the maturation of these cysteine proteases by a serine protease and while they are successfully targeted to the cuticle interfaces in its absence the cysteine proteases may not be fully active and thus molting is inhibited.

The expression of the *Ov-spi* transcripts in the other lifecycle stages of *O. volvulus* suggests they have functions outside of molting. The native proteins were also immunolocalized to the eggshells surrounding developing embryos within the uterus of adult female worms, and to

[5] Y. Oksov, unpublished observation.
[6] S. Lustigman and C. Poole, unpublished data.

sperm within the testis of adult male worms suggesting a role in embryogenesis, microfilarial development, and spermatogenesis. *Bm-spi-1* is also expressed in a variety of lifecycle stages suggesting that these inhibitors may have similar multifunctional roles in the other filariae. The *A. suum* chymotrypsin/elastase inhibitors have been localized to the eggs, egg-shell-derived sheath of the L2 stages, and sperm, either through specific antibodies or treatment with fluorescently labeled proteases (89, 90). However, these studies did not address whether or not the *A. suum* inhibitors were also inhibiting endogenous nematode proteases participating in the tissue remodeling processes taking place in the developing embryos. Although we do not know what functions the *Ov*-SPIs have in nematode sperm, another TIL domain-containing protein has been identified as a component of the seminal fluid of *D. melanogaster* (60) suggesting TILs might have conserved functions in sperm biology. Serine proteases are known to be involved in embryonic development (91) in a variety of organisms. In *C. elegans*, blisterases have been shown to be involved in early development of the nematodes as well as in cuticle formation (reviewed in Refs. 72–74). It is possible that there are targets of the *Ov*-SPIs in the adults as well as the molting larvae.

Moreover, it is possible that, like other previously characterized nematode protease inhibitors, such as the cystatin family (29, 30) and the serpin family of serine protease inhibitors (27, 28, 92), the *Ov*-SPIs have exogenous as well as endogenous functions during the lifecycle of the parasite. This could involve the control of both host and parasite ectoproteases. Filarial cystatins have been shown to have immunomodulatory properties either through direct effects on immune cell activation or by blocking antigen processing and presentation on class II major histocompatibility complex (29, 93–98). Nippocystatin, a cysteine protease inhibitor from *Nippostrongylus brasiliensis*, was also shown to inhibit antigen processing and modulate antigen-specific immune responses to the parasite (99). Serine protease inhibitors belonging to the serpin family, such as viral serpins (100–102), have also been implicated in immunomodulation. A filarial serpin identified in *B. malayi* (26) acts as a major T cell antigen (103), whereas a serpin from the intestinal nematode *Trichostrongylus vitrinus* inhibits host serine proteases (104). We are currently exploring the immunomodulatory properties of the *Ov*-SPIs and their ability to specifically inhibit proteases released from activated neutrophils and monocytes, such as elastase and cathepsin G (reviewed in Refs. 105 and 106), which may be involved in the control of inflammation (107, 108). Neutrophils have been found to be important effector cells in the killing of *O. volvulus* larvae (109, 110). They are also involved in the pathology associated with nodule formation around adult *Onchocerca* worms (111), microfilaria-mediated ocular pathology (112, 113), and are involved in the immune responses generated after anti-filarial treatment (114, 115). Control of proteases released from these cells would be vital for establishment and long term survival of the parasites within the host.

Indirect evidence of the involvement of the *Ov*-SPIs in immune regulation is that *Ov*-SPIs are antigenic and highly recognized by individuals exposed to *O. volvulus* indicating exposure to the inhibitor,[7] and thus suggesting that they are released from the parasite during the early stages of parasite establishment in the host. Interestingly, antibody responses to *Ov*-SPIs are higher in putatively immune individuals when compared with age-matched infected individuals, and the responses are up-regulated with age in chronically infected individuals[7] suggesting a role in protective immunity. *Ov*-SPI-1 is one of the vaccine candidates against *O. volvulus*.

[7] L. Ford and S. Lustigman, unpublished data.

In conclusion, we have identified a novel filarial serine protease inhibitor family with potential multifunctional roles in the development of the parasite, including molting, establishment in the final host, embryogenesis, and reproduction. Future work will focus on identifying the one or more potential target enzymes for the filarial serine protease inhibitors, including both endogenous parasite and exogenous host serine proteases. Identification of their target proteases may be important in the identification of potential targets for drug and vaccine development as well as providing further information on the biology of molting and adult reproductive processes in nematodes.

Acknowledgments—We thank Drs. Sarwar Hashmi and Jun Zhang from the Laboratory of Molecular Parasitology, New York Blood Center (NYBC), for expert technical assistance and advice, Dr. Cheryl Lobo and Marilis Rodriguez for the Pf-eba-140 construct and primers, and Michal Tarnawski for assistance with figures. We also thank Dr. David Abraham, at the Department of Microbiology and Immunology, Thomas Jefferson University, Philadelphia, for the production of mouse polyclonal antibodies. We thank The Filarial Genome Project Resource Center, Smith College, Northampton, MA; Claire Whitton in the Blaxter laboratory, University of Edinburgh, Edinburgh, UK; and Genome Sequencing Center, Washington University, for supplying the cDNA libraries and EST clones. For DNA sequencing we thank Susan Fetics and Gitanjali Patel of the Nucleic Acid Analysis Laboratory, NYBC.

REFERENCES

1. Page, A. P. (2001) in *Parasitic Nematodes: Molecular Biology, Biochemistry and Immunology* (Kennedy, M. H., and Harnett, W., eds) pp. 167–186, CABI Publishing, Oxon, UK
2. Lustigman, S. (1993) *Parasitol. Today* **9,** 294–297
3. Davey, K. G., and Kan, S. P. (1968) *Can. J. Zool.* **46,** 893–898
4. Hotez, P., Haggerty, J., Hawdon, J., Milstone, L., Gamble, H. R., Schad, G., and Richards, F. (1990) *Infect. Immun.* **58,** 3883–3892
5. Gamble, H. R., Purcell, J. P., and Fetterer, R. H. (1989) *Mol. Biochem. Parasitol.* **33,** 49–58
6. Richer, J. K., Sakanari, J. A., Frank, G. R., and Grieve, R. B. (1992) *Exp. Parasitol.* **75,** 213–222
7. Hong, X., Bouvier, J., Wong, M. M., Yamagata, G. Y., and McKerrow, J. H. (1993) *Exp. Parasitol.* **76,** 127–133
8. Suzuki, M., Sagoh, N., Iwasaki, H., Inoue, H., and Takahashi, K. (2004) *Biol. Chem.* **385,** 565–568
9. Davis, M. W., Birnie, A. J., Chan, A. C., Page, A. P., and Jorgensen, E. M. (2004) *Development* **131,** 6001–6008
10. Lustigman, S., McKerrow, J. H., Shah, K., Lui, J., Huima, T., Hough, M., and Brotman, B. (1996) *J. Biol. Chem.* **271,** 30181–30189
11. Zhan, B., Hotez, P. J., Wang, Y., and Hawdon, J. M. (2002) *Mol. Biochem. Parasitol.* **120,** 291–296
12. Lizotte-Waniewski, M., Tawe, W., Guiliano, D. B., Lu, W., Liu, J., Williams, S. A., and Lustigman, S. (2000) *Infect. Immun.* **68,** 3491–3501
13. Parkinson, J., Mitreva, M., Whitton, C., Thomson, M., Daub, J., Martin, J., Schmid, R., Hall, N., Barrell, B., Waterston, R. H., McCarter, J. P., and Blaxter, M. L. (2004) *Nat. Genet.* **36,** 1259–1267
14. Hashmi, S., Britton, C., Liu, J., Guiliano, D. B., Oksov, Y., and Lustigman, S. (2002) *J. Biol. Chem.* **277,** 3477–3486
15. Guiliano, D. B., Hong, X., McKerrow, J. H., Blaxter, M. L., Oksov, Y., Liu, J., Ghedin, E., and Lustigman, S. (2004) *Mol. Biochem. Parasitol.* **136,** 227–242
16. Babin, D. R., Peanasky, R. J., and Goos, S. M. (1984) *Arch. Biochem. Biophys.* **232,** 143–161
17. Stassens, P., Bergum, P. W., Gansemans, Y., Jespers, L., Laroche, Y., Huang, S., Maki, S., Messens, J., Lauwereys, M., Cappello, M., Hotez, P. J., Lasters, I., and Vlasuk, G. P. (1996) *Proc. Natl. Acad. Sci. U. S. A.* **93,** 2149–2154
18. Peanasky, R. J., Bentz, Y., Paulson, B., Graham, D. L., and Babin, D. R. (1984) *Arch. Biochem. Biophys.* **232,** 127–134
19. Hawley, J. H., and Peanasky, R. J. (1992) *Exp. Parasitol.* **75,** 112–118
20. Morris, S. R., and Sakanari, J. A. (1994) *J. Biol. Chem.* **269,** 27650–27656
21. Rhoads, M. L., Fetterer, R. H., and Hill, D. E. (2000) *Exp. Parasitol.* **94,** 1–7
22. Chu, D., Bungiro, R. D., Ibanez, M., Harrison, L. M., Campodonico, E., Jones, B. F., Mieszczanek, J., Kuzmic, P., and Cappello, M. (2004) *Infect. Immun.* **72,** 2214–2221
23. Cappello, M., Vlasuk, G. P., Bergum, P. W., Huang, S., and Hotez, P. J. (1995) *Proc. Natl. Acad. Sci. U. S. A.* **92,** 6152–6156
24. Harrison, L. M., Nerlinger, A., Bungiro, R. D., Cordova, J. L., Kuzmic, P., and Cap-

pello, M. (2002) *J. Biol. Chem.* **277,** 6223–6229
25. Mieszczanek, J., Harrison, L. M., and Cappello, M. (2004) *Mol. Biochem. Parasitol.* **137,** 151–159
26. Yenbutr, P., and Scott, A. L. (1995) *Infect. Immun.* **63,** 1745–1753
27. Zang, X., and Maizels, R. M. (2001) *Trends Biochem. Sci.* **26,** 191–197
28. Maizels, R. M., Gomez-Escobar, N., Gregory, W. F., Murray, J., and Zang, X. (2001) *Int. J. Parasitol.* **31,** 889–898
29. Hartmann, S., and Lucius, R. (2003) *Int. J. Parasitol.* **33,** 1291–1302
30. Lustigman, S., Brotman, B., Huima, T., Prince, A. M., and McKerrow, J. H. (1992) *J. Biol. Chem.* **267,** 17339–17346
31. Altschul, S. F., Madden, T. L., Schaffer, A. A., Zhang, J., Zhang, Z., Miller, W., and Lipman, D. J. (1997) *Nucleic Acids Res.* **25,** 3389–3402
32. Thompson, J. D., Gibson, T. J., Plewniak, F., Jeanmougin, F., and Higgins, D. G. (1997) *Nucleic Acids Res.* **25,** 4876–4882
33. Bateman, A., Coin, L., Durbin, R., Finn, R. D., Hollich, V., Griffiths-Jones, S., Khanna, A., Marshall, M., Moxon, S., Sonnhammer, E. L., Studholme, D. J., Yeats, C., and Eddy, S. R. (2004) *Nucleic Acids Res.* **32,** D138–D141
34. Letunic, I., Copley, R. R., Schmidt, S., Ciccarelli, F. D., Doerks, T., Schultz, J., Ponting, C. P., and Bork, P. (2004) *Nucleic Acids Res.* **32,** D142–D144
35. Rawlings, N. D., Tolle, D. P., and Barrett, A. J. (2004) *Biochem. J.* **378,** 705–716
36. C. elegans Sequencing Consortium (1998) *Science* **282,** 2012–2018
37. Swofford, D. L., Olsen, G. J., Waddell, P. J., and Hillis, D. M. (1996) in *Molecular Systematics* (Hillis, D. M., Moritz, C., and Mable, B. K., eds) 2nd Ed., pp. 407–514, Sinauer, Sunderland, MA
38. Huelsenbeck, J. P., and Bollback, J. P. (2001) *Syst. Biol.* **50,** 351–366
39. Blaxter, M. L., De Ley, P., Garey, J. R., Liu, L. X., Scheldeman, P., Vierstraete, A., Vanfleteren, J. R., Mackey, L. Y., Dorris, M., Frisse, L. M., Vida, J. T., and Thomas, W. K. (1998) *Nature* **392,** 71–75
40. Huang, K., Strynadka, N. C., Bernard, V. D., Peanasky, R. J., and James, M. N. (1994) *Structure* **2,** 679–689
41. Sali, A., and Blundell, T. L. (1993) *J. Mol. Biol.* **234,** 779–815
42. Laskowski, R. A., MacArthur, M. W., Moss, D. S., and Thornton, J. M. (1993) *J. Appl. Crystallogr.* **26,** 283–291
43. Abraham, D., Leon, O., Leon, S., and Lustigman, S. (2001) *Infect. Immun.* **69,** 262–270
44. Joseph, G. T., McCarthy, J. S., Huima, T., Mair, K. F., Kass, P. H., Boussinesq, M., Goodrick, L., Bradley, J. E., and Lustigman, S. (1997) *Mol. Biochem. Parasitol.* **90,** 55–68
45. Lustigman, S., Brotman, B., Huima, T., and Prince, A. M. (1991) *Mol. Biochem. Parasitol.* **45,** 65–75
46. Lustigman, S., Zhang, J., Lui, J., Oksov, Y., and Hashmi, S. (2004) *Mol. Biochem. Parasitol.* **138,** 165–170
47. Hashmi, S., Zhang, J., Oksov, Y., and Lustigman, S. (2004) *J. Biol. Chem.* **279,** 6035–6045
48. Comley, J. C., Townson, S., Rees, M. J., and Dobinson, A. (1989) *Trop. Med. Parasitol.* **40,** 311–316
49. Lustigman, S., Brotman, B., Huima, T., Castelhano, A. L., Singh, R. N., Mehta, K., and Prince, A. M. (1995) *Antimicrob. Agents Chemother.* **39,** 1913–1919
50. Schechter, I., and Berger, A. (1967) *Biochem. Biophys. Res. Commun.* **27,** 157–162
51. Peanasky, R. J., Bentz, Y., Homandberg, G. A., Minor, S. T., and Babin, D. R. (1984) *Arch. Biochem. Biophys.* **232,** 135–142
52. Nguyen, T. T., Qasim, M. A., Morris, S., Lu, C. C., Hill, D., Laskowski, M., Jr., and Sakanari, J. A. (1999) *Mol. Biochem. Parasitol.* **102,** 79–89
53. Goodman, R. B., Martzen, M. R., and Peanasky, R. J. (1983) *Acta Biochim. Pol.* **30,** 233–244
54. Goodman, R. B., and Peanasky, R. J. (1982) *Anal. Biochem.* **120,** 387–393
55. Parkinson, J., Whitton, C., Schmid, R., Thomson, M., and Blaxter, M. (2004) *Nucleic Acids Res.* **32,** D427–D430
56. Lu, C. C., Nguyen, T., Morris, S., Hill, D., and Sakanari, J. A. (1998) *Exp. Parasitol.* **89,** 257–261
57. Rhoads, M. L., Fetterer, R. H., Hill, D. E., and Urban, J. F., Jr. (2000) *Exp. Parasitol.* **95,** 36–44
58. Bania, J., Stachowiak, D., and Polanowski, A. (1999) *Eur. J. Biochem.* **262,** 680–687
59. Polanowski, A., Wilusz, T., Blum, M. S., Escoubas, P., Schmidt, J. O., and Travis, J. (1992) *Comp. Biochem. Physiol. B* **102,** 757–760
60. Lung, O., Tram, U., Finnerty, C. M., Eipper-Mains, M. A., Kalb, J. M., and Wolfner, M. F. (2002) *Genetics* **160,** 211–224
61. Parkinson, N. M., Conyers, C., Keen, J., MacNicoll, A., Smith, I., Audsley, N., and Weaver, R. (2004) *Insect. Biochem. Mol. Biol.* **34,** 565–571
62. Zhu, S., and Li, W. (2002) *Comp. Biochem. Physiol. B Biochem. Mol. Biol.* **131,** 749–756
63. Mignogna, G., Pascarella, S., Wechselberger, C., Hinterleitner, C., Mollay, C., Amiconi, G., Barra, D., and Kreil, G. (1996) *Protein Sci.* **5,** 357–362
64. Ali, M. F., Lips, K. R., Knoop, F. C., Fritzsch, B., Miller, C., and Conlon, J. M. (2002) *Biochim. Biophys. Acta* **1601,** 55–63
65. Hardy, D. M., and Garbers, D. L. (1995) *J. Biol. Chem.* **270,** 26025–26028
66. Bonthron, D., Orr, E. C., Mitsock, L. M., Ginsburg, D., Handin, R. I., and Orkin, S. H. (1986) *Nucleic Acids Res.* **14,** 7125–7127
67. McKerrow, J. H., Huima, T., and Lustigman, S. (1999) *Parasitol. Today* **15,** 123
68. Sakanari, J. A., Staunton, C. E., Eakin, A. E., Craik, C. S., and McKerrow, J. H. (1989) *Proc. Natl. Acad. Sci. U. S. A.* **86,** 4863–4867
69. Nagano, I., Wu, Z., Nakada, T., Boonmars, T., and Takahashi, Y. (2003) *J. Parasitol.* **89,** 92–98
70. Romaris, F., North, S. J., Gagliardo, L. F., Butcher, B. A., Ghosh, K., Beiting, D. P., Panico, M., Arasu, P., Dell, A., Morris, H. R., and Appleton, J. A. (2002) *Mol. Biochem. Parasitol.* **122,** 149–160
71. Haffner, A., Guilavogui, A. Z., Tischendorf, F. W., and Brattig, N. W. (1998) *Exp. Parasitol.* **90,** 26–33
72. Thacker, C., Peters, K., Srayko, M., and Rose, A. M. (1995) *Genes Dev.* **9,** 956–971
73. Thacker, C., and Rose, A. M. (2000) *BioEssays* **22,** 545–553
74. Peters, K., McDowall, J., and Rose, A. M. (1991) *Genetics* **129,** 95–102
75. Jin, J., Poole, C. B., Slatko, B. E., and McReynolds, L. A. (1999) *Gene* (*Amst.*) **237,** 161–175
76. Poole, C. B., Jin, J., and McReynolds, L. A. (2003) *J. Biol. Chem.* **278,** 36183–36190
77. Frand, A. R., Russel, S., and Ruvkun, G. (2005) *PLoS Biol.* **3,** e312
78. Lackey, A., James, E. R., Sakanari, J. A., Resnick, S. D., Brown, M., Bianco, A. E., and McKerrow, J. H. (1989) *Exp. Parasitol.* **68,** 176–185
79. Rayburn, L. Y., Gooding, H. C., Choksi, S. P., Maloney, D., Kidd, A. R., 3rd, Siekhaus, D. E., and Bender, M. (2003) *Genetics* **163,** 227–237
80. Jakobsen, R. K., Ono, S., Powers, J. C., and Delotto, R. (2005) *Histochem. Cell Biol.* **123,** 51–60
81. Jones, G., Venkataraman, V., and Manczak, M. (1993) *Insect. Biochem. Mol. Biol.* **23,** 825–829
82. Samuels, R. I., Charnley, A. K., and Reynolds, S. E. (1993) *Insect Biochem. Mol. Biol* **23,** 607–614
83. Cole, S. C. J., Charnley, A. K., and Cooper, R. M. (1993) *FEMS Microbiol. Lett.* **113,** 189–195
84. Samuels, R. I., and Paterson, I. C. (1995) *Comp. Biochem. Physiol. B Biochem. Mol. Biol.* **110,** 661–669
85. Kress, H., Jarrin, A., Thuroff, E., Saunders, R., Weise, C., Schmidt am Busch, M., Knapp, E. W., Wedde, M., and Vilcinskas, A. (2004) *Insect. Biochem. Mol. Biol.* **34,** 855–869
86. Jackson, A. L., and Linsley, P. S. (2004) *Trends Genet.* **20,** 521–524
87. Jackson, A. L., Bartz, S. R., Schelter, J., Kobayashi, S. V., Burchard, J., Mao, M., Li, B., Cavet, G., and Linsley, P. S. (2003) *Nat. Biotechnol.* **21,** 635–637
88. Unnasch, T. R., and Williams, S. A. (2000) *Int. J. Parasitol.* **30,** 543–552
89. Martzen, M. R., Geise, G. L., Hogan, B. J., and Peanasky, R. J. (1985) *Exp. Parasitol.* **60,** 139–149
90. Martzen, M. R., Geise, G. L., and Peanasky, R. J. (1986) *Exp. Parasitol.* **61,** 138–145
91. Krem, M. M., and Cera, E. D. (2002) *Trends Biochem. Sci.* **27,** 67–74
92. Maizels, R. M., Blaxter, M. L., and Scott, A. L. (2001) *Parasite Immunol.* **23,** 327–344
93. Manoury, B., Gregory, W. F., Maizels, R. M., and Watts, C. (2001) *Curr. Biol.* **11,** 447–451
94. Schonemeyer, A., Lucius, R., Sonnenburg, B., Brattig, N., Sabat, R., Schilling, K., Bradley, J., and Hartmann, S. (2001) *J. Immunol.* **167,** 3207–3215
95. Hartmann, S., Schonemeyer, A., Sonnenburg, B., Vray, B., and Lucius, R. (2002) *Parasite Immunol.* **24,** 253–262
96. Schierack, P., Lucius, R., Sonnenburg, B., Schilling, K., and Hartmann, S. (2003) *Infect. Immun.* **71,** 2422–2429
97. Pfaff, A. W., Schulz-Key, H., Soboslay, P. T., Taylor, D. W., MacLennan, K., and Hoffmann, W. H. (2002) *Int. J. Parasitol.* **32,** 171–178
98. Murray, J., Manoury, B., Balic, A., Watts, C., and Maizels, R. M. (2005) *Mol. Biochem. Parasitol.* **139,** 197–203
99. Dainichi, T., Maekawa, Y., Ishii, K., Zhang, T., Nashed, B. F., Sakai, T., Takashima, M., and Himeno, K. (2001) *Infect. Immun.* **69,** 7380–7386
100. Macen, J. L., Upton, C., Nation, N., and McFadden, G. (1993) *Virology* **195,** 348–363
101. Ray, C. A., Black, R. A., Kronheim, S. R., Greenstreet, T. A., Sleath, P. R., Salvesen, G. S., and Pickup, D. J. (1992) *Cell* **69,** 597–604
102. Kettle, S., Alcami, A., Khanna, A., Ehret, R., Jassoy, C., and Smith, G. L. (1997) *J. Gen. Virol.* **78,** 677–685
103. Zang, X., Atmadja, A. K., Gray, P., Allen, J. E., Gray, C. A., Lawrence, R. A., Yazdanbakhsh, M., and Maizels, R. M. (2000) *J. Immunol.* **165,** 5161–5169
104. MacLennan, K., McLean, K., and Knox, D. P. (2005) *Parasitology* **130,** 349–357
105. Caughey, G. H. (1994) *Am. J. Respir. Crit. Care Med.* **150,** S138–S142
106. Owen, C. A., and Campbell, E. J. (1999) *J. Leukoc. Biol.* **65,** 137–150
107. Bank, U., and Ansorge, S. (2001) *J. Leukoc. Biol.* **69,** 197–206
108. Steinhoff, M., Buddenkotte, J., Shpacovitch, V., Rattenholl, A., Moormann, C., Vergnolle, N., Luger, T. A., and Hollenberg, M. D. (2005) *Endocr. Rev.* **26,** 1–43

109. Johnson, E. H., Irvine, M., Kass, P. H., Browne, J., Abdullai, M., Prince, A. M., and Lustigman, S. (1994) *Trop. Med. Parasitol.* **45,** 331–335
110. Greene, B. M., Taylor, H. R., and Aikawa, M. (1981) *J. Immunol.* **127,** 1611–1618
111. Gallin, M. Y., Jacobi, A. B., Buttner, D. W., Schonberger, O., Marti, T., and Erttmann, K. D. (1995) *J. Exp. Med.* **182,** 41–47
112. Pearlman, E., Hall, L. R., Higgins, A. W., Bardenstein, D. S., Diaconu, E., Hazlett, F. E., Albright, J., Kazura, J. W., and Lass, J. H. (1998) *Invest. Ophthalmol. Vis. Sci.* **39,** 1176–1182
113. Hall, L. R., and Pearlman, E. (1999) *Clin. Microbiol. Rev.* **12,** 445–453
114. Gutierrez-Pena, E. J., Knab, J., and Buttner, D. W. (1996) *Parasitology* **113,** 403–414
115. Njoo, F. L., Hack, C. E., Oosting, J., Stilma, J. S., and Kijlstra, A. (1993) *Clin. Exp. Immunol.* **94,** 330–333

Characterization of a Novel Filarial Serine Protease Inhibitor, *Ov*-SPI-1, from *Onchocerca volvulus*, with Potential Multifunctional Roles during Development of the Parasite

Louise Ford, David B. Guiliano, Yelena Oksov, Asim K. Debnath, Jing Liu, Steven A. Williams, Mark L. Blaxter and Sara Lustigman

J. Biol. Chem. 2005, 280:40845-40856.
doi: 10.1074/jbc.M504434200 originally published online September 26, 2005
